Article

Current Biology

Zyxin Antagonizes the FERM Protein Expanded to Couple F-Actin and Yorkie-Dependent Organ Growth

Graphical Abstract

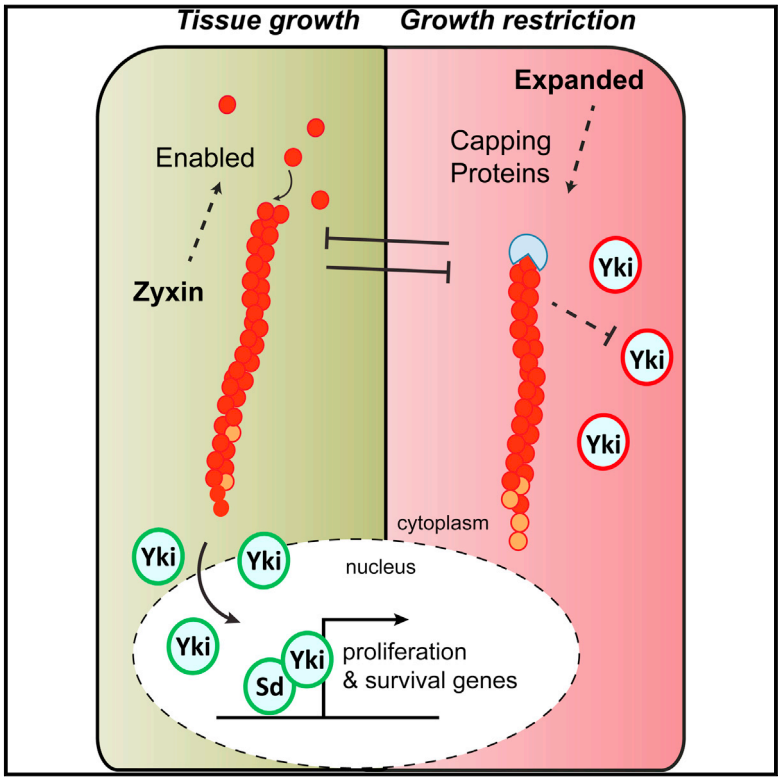

Highlights

- Zyx antagonizes Ex to control growth, eye differentiation, and F-actin
- Membrane targeting of Zyx promotes tissue growth and Yki activity
- Zyx modulates Yki target gene expression and the interaction of Sd with Yki
- The Ena-binding region of Zyx is required to antagonize Ex function

Authors

Pedro Gaspar, Maxine V. Holder, ..., Florence Janody, Nicolas Tapon

Correspondence

fjanody@igc.gulbenkian.pt (F.J.), nic.tapon@cancer.org.uk (N.T.)

In Brief

Gaspar et al. describe a cytoskeletal mechanism that finely regulates tissue growth, based on the antagonism between Zyxin/Ena, which promotes tissue and actin filament growth, and Expanded/Capping Protein, which antagonizes these processes. This mechanism modulates the activity of the Yorkie/YAP oncogene, the downstream effector of the Hippo pathway.

Gaspar et al., 2015, Current Biology *25*, 679–689
March 16, 2015
http://dx.doi.org/10.1016/j.cub.2015.01.010

Current Biology 25, 679–689, March 16, 2015 ©2015 Elsevier Ltd All rights reserved http://dx.doi.org/10.1016/j.cub.2015.01.010

Article

Zyxin Antagonizes the FERM Protein Expanded to Couple F-Actin and Yorkie-Dependent Organ Growth

Pedro Gaspar,[1,2] Maxine V. Holder,[1] Birgit L. Aerne,[1] Florence Janody,[2,*] and Nicolas Tapon[1,*]
[1]Apoptosis and Proliferation Control Laboratory, Cancer Research UK, London Research Institute, 44 Lincoln's Inn Fields, London WC2A 3LY, UK
[2]Instituto Gulbenkian de Ciência, Rua da Quinta Grande 6, 2780-156 Oeiras, Portugal

Summary

Background: Coordinated multicellular growth during development is achieved by the sensing of spatial and nutritional boundaries. The conserved Hippo (Hpo) signaling pathway has been proposed to restrict tissue growth by perceiving mechanical constraints through actin cytoskeleton networks. The actin-associated LIM proteins Zyxin (Zyx) and Ajuba (Jub) have been linked to the control of tissue growth via regulation of Hpo signaling, but the study of Zyx has been hampered by a lack of genetic tools.
Results: We generated a *zyx* mutant in *Drosophila* using TALEN endonucleases and used this to show that Zyx antagonizes the FERM-domain protein Expanded (Ex) to control tissue growth, eye differentiation, and F-actin accumulation. Zyx membrane targeting promotes the interaction between the transcriptional co-activator Yorkie (Yki) and the transcription factor Scalloped (Sd), leading to activation of Yki target gene expression and promoting tissue growth. Finally, we show that Zyx's growth-promoting function is dependent on its interaction with the actin-associated protein Enabled (Ena) via a conserved LPPPP motif and is antagonized by Capping Protein (CP).
Conclusions: Our results show that Zyx is a functional antagonist of Ex in growth control and establish a link between actin filament polymerization and Yki activity.

Introduction

The control of tissue size represents a major unsolved question in developmental biology. The conserved Hippo (Hpo) signaling pathway is thought to sense mechanical and nutritional cues to restrict tissue growth [1]. Activation of the Ste20-like kinase Hpo (MST1/2 in mammals) and subsequent phosphorylation of the downstream Ndr-like kinase Warts (Wts-LATS1/2 in mammals) inhibits the transcriptional co-activator Yorkie (Yki-YAP/TAZ in mammals), via phosphorylation at S168. This prevents the interaction of Yki with transcription factor partners, such as Scalloped (Sd-TEAD1-4 in mammals), thereby inhibiting expression of pro-growth and survival genes [1].

The known upstream stimuli for Hpo signaling involve a number of regulatory proteins, many of which are associated with the actin cytoskeleton [2]. In particular, the *Drosophila* proteins Expanded (Ex) and Merlin (Mer), which belong to the FERM (Four point one, Ezrin, Radixin, Moesin) domain family, and the protocadherins Fat (Ft) and Dachsous (Ds), were identified as tumor suppressors that prevent expression of Yki target genes [3–8]. Whether Ex/Mer and Ft/Ds signaling represent entirely distinct branches of Hpo signaling remains unclear. For instance, Ft depletion leads to a reduction in apical Ex localization [6–8]. However, Ft and Ex have been implicated in distinct functions: Ft/Ds are involved in the control of planar cell polarity (PCP) [9, 10], while Ex has strong effects on eye differentiation [11–15]. The proposed mechanisms of Ft and Ex function are also distinct. In particular, Ex promotes cytoplasmic sequestration of Yki through direct binding and by promoting Hpo-Wts kinase activity [16, 17], while Ft antagonizes the growth-promoting function of the atypical myosin Dachs (D), which, in turn, destabilizes Wts [4].

Several reports have highlighted the contribution of the actin cytoskeleton to Hpo signaling [18]. The actin Capping Protein $\alpha\beta$ heterodimer (CP), which prevents addition of actin monomers to F-actin barbed ends, antagonizes Yki activity, and thereby restricts tissue growth [19, 20]. Accordingly, in mammals, CapZ and other factors that restrict F-actin levels, have growth-restrictive effects via the control of YAP/TAZ subcellular localization, particularly in response to mechanical cues [21]. Interestingly, YAP and TAZ respond to mechanical cues dependent on actomyosin networks and formin-dependent actin polymerization [22–24]. Recently, the actin-associated LIM (Lin11, Isl-1, and Mec-3) domain protein Zyxin (Zyx) has been shown to mediate the effects of Ft-Ds signaling on Yki target genes, by promoting Wts destabilization via its interaction with D [25]. Importantly, Zyx provides a link to the actin polymerization machinery, since it directly interacts with the actin-binding proteins Enabled (Ena)/VASP via conserved F/LPPPP motifs, and promotes Ena function in barbed-end F-actin polymerization [26–29].

The analysis of *Drosophila zyx* has been limited by the absence of a mutant. Here, we generate a *zyx* mutation and describe its effects on growth and Hpo signaling. We show that Zyx strongly antagonizes Ex function in growth control, eye differentiation and F-actin accumulation, while being largely dispensable for Ft-mediated tissue growth. Finally, our work suggests that Zyx's growth-promoting function requires its ability to bind the actin polymerization factor Ena.

Results

Zyx Is Not Required for Viability but Promotes Tissue Growth

Analysis of *zyx* function has relied on the use of transgenic RNAi. To investigate the role of *zyx* in Hpo signaling, we generated a *zyx* mutant allele by TALEN (Transcription activator-like effector nuclease)-mediated mutagenesis. Using a TALEN pair that targets the first common exon of all *zyx* splice variants, we generated a founder mutation ($zyx^{\Delta 41}$), carrying a 7-bp deletion (Figure 1A). This mutation induces a frameshift at codon 103 (isoforms RA and RB), 41 (isoform RG), or 14 (isoform RH), resulting in a premature stop codon leading to a 19- to 108-amino-acid peptide, lacking most of the Zyx sequence (Figure 1A). An antibody against Zyx revealed a band of

*Correspondence: fjanody@igc.gulbenkian.pt (F.J.), nic.tapon@cancer.org.uk (N.T.)

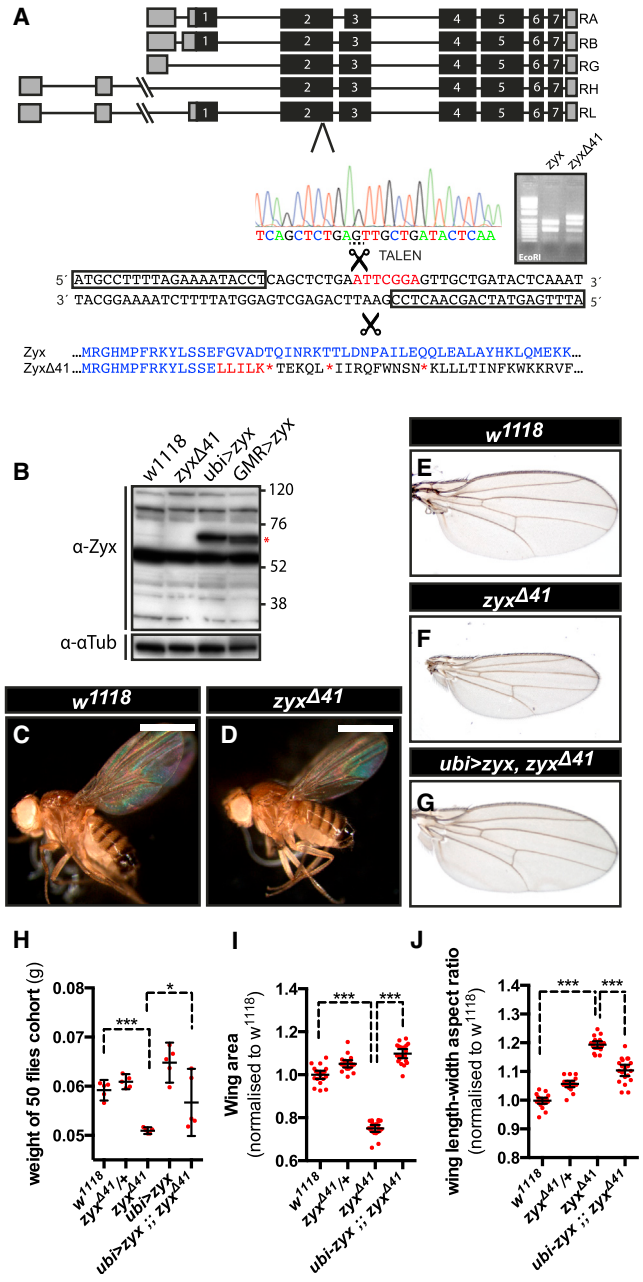

Figure 1. Loss of *zyx* Restricts Tissue Growth

(A) *zyx* gene model and mutagenesis schematic using TALEN endonucleases. The $zyx^{\Delta 41}$ allele is identified by the DNA sequence chromatogram and failure of EcoRI digestion. Expected protein sequence shown in blue. The deleted 7-bp DNA sequence and resulting protein frameshift are shown in red.

(B) Western blot on adult fly extracts from w^{1118} (lane 1), $zyx^{\Delta 41}$ mutants (lane 2), or flies expressing *zyx* under the *ubi-p63E* promoter (lane 3) or *GMR*-Gal4 control (lane 4), blotted with anti-Zyx (upper blot) and anti-α-tubulin (lower blot).

(C and D) Adult w^{1118} (C) or $zyx^{\Delta 41}$ (D) flies. Scale bars, 0.5 mm.

(E–G) Female wings homozygous for w^{1118} (E), $zyx^{\Delta 41}$ (F), or expressing *zyx* under the control of the *ubip63E* promoter (G).

(H) Quantification of adult dry weight for indicated genotypes (n ≥ 5).

(I) Quantification of adult wing area normalized to w^{1118} for indicated genotypes (n ≥ 20).

(J) Quantification of aspect ratio between length of vein 5 and length between tips of vein 2 and 4 for indicated genotypes (n ≥ 20).

Data are shown as scatterplot with mean values ± SD with ***p < 0.0001, **p < 0.005, *p < 0.05 for this and all subsequent figures.

approximately 65 kDa in lysates of control adult animals, which was increased in lysates from adults overexpressing *zyx* ubiquitously or with the *GMR-Gal4* driver and lost in $zyx^{\Delta 41}$ adult animals, suggesting that $zyx^{\Delta 41}$ represents a null allele (Figure 1B).

$zyx^{\Delta 41}$ homozygous mutant animals were viable and fertile. However, adults were smaller than control wild-type animals (isogenic w^{1118}) (Figures 1C and 1D). Quantification of this defect showed that $zyx^{\Delta 41}$ adult animals displayed a significant decrease in body weight (Figure 1H) and had smaller (Figures 1E, 1F, and 1I) and narrower wings (Figures 1E, 1F, and 1J). These defects resulted from the loss of *zyx,* as re-expressing a full-length *zyx cDNA* ubiquitously (*ubi > zyx)* in $zyx^{\Delta 41}$ animals restored normal adult weight (Figure 1H), wing size (Figures 1G and 1I), and shape (Figures 1G and 1J). Thus, *zyx* is not required for survival but is required for normal tissue growth.

Zyx Is Required for Phenotypes Elicited by Ex Loss

We analyzed the effects of *zyx* loss combined with inactivation of Hpo pathway components. Removing *zyx* function did not significantly affect the number of interommatidial cells (IOCs) in the pupal retina, a common readout of Hpo pathway activity (Figures 2A, 2B, and 2I; Table S1), nor adult eye size (Figures 2J–2K′), nor photoreceptor differentiation, as visualized using the neuronal marker ELAV in third instar eye discs (Figures S1E and S1F). Thus, *zyx* is dispensable for normal eye development. We then generated mutant eyes for Hpo pathway components using the EGUF (*ey-GAL4/UAS-FLP/GMR-hid*) method [30]. As expected, single EGUF mutant retinas for *ft* (Figures 2C and 2I), *ex* (Figures 2E and 2I), or *hpo* (Figures 2G and 2I) showed a significant increase in the number of IOCs compared to wild-type retinas (w^{1118}) (Figures 2A and 2I; Table S1).

Removing *zyx* function slightly reduced the supernumerary IOC phenotype of $ft^{G\text{-}rv}$ mutant retinas (Figures 2C, 2D, and 2I; Table S1) but did not affect the size of these mutant eyes (Figures 2L–2M′). Additionally, ft^{8}, $zyx^{\Delta 41}$ double-mutant retinas did not show significant changes in IOC number compared to ft^{8} single-mutant retinas (Figure 2I; Figures S1A and S1B; Table S1). Moreover, loss of *zyx* did not improve survival of $ft^{8}/ft^{G\text{-}rv}$ transheterozygous larvae to third instar (Figure S1U), restore their reduced number of photoreceptor cells (Figures S1G and S1H), or rescue the overgrowth of their wing discs (Figures S1M and S1N). Therefore, *zyx* function is not essential to promote tissue overgrowth upon *ft* loss, suggesting a function for *zyx* independent of Ft-Ds signaling. Consistent with these observations, d^{GC13}, $zyx^{\Delta 41}$ double-mutant adult eyes or eye and wing discs were much smaller than those in d^{GC13} single mutants (Figures 2N–2O′, S1I, S1J, S1O, and S1P), indicating that *zyx* has *d*-independent functions in growth control.

Strikingly, removing *zyx* function suppressed the supernumerary IOCs of ex^{e1} or ex^{AP50} mutant retinas (Figures 2E, 2F, 2I, S1C, and S1D; Table S1), restored the size of ex^{e1} eyes (Figures 2P–2Q′), and recovered ELAV-positive photoreceptor cells of third instar ex^{e1} eye discs (Figures S1K and S1L). Moreover, loss of *zyx* visibly suppressed the wing disc overgrowth of ex^{e1}/ex^{AP50} animals (Figures S1Q and S1R) and restored viability of ex^{e1} animals to the adult stage (16% survival; Figure S1U). This shows that *zyx* function is required for eye and wing overgrowth and defects in eye differentiation caused by *ex* loss.

$hpo^{5.1}$, $zyx^{\Delta 41}$ double-mutant retinas showed a moderate but significant decrease in IOC number compared to $hpo^{5.1}$

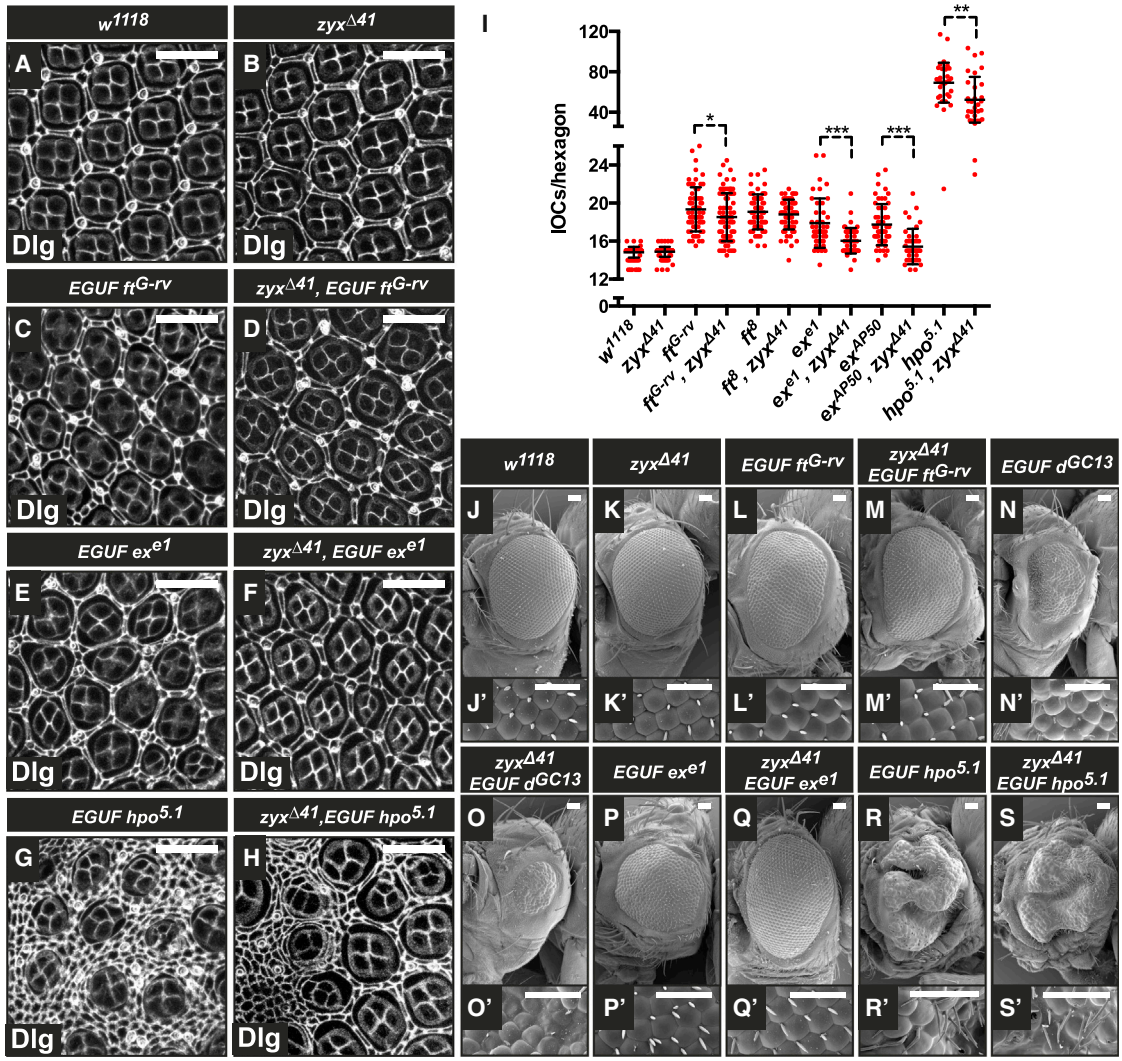

Figure 2. Removing *zyx* Function Suppresses Eye Defects Induced by Loss of *ex*

(A–H and J–S′) Female 40-hr retinas (A–H) or adult eyes (J–S′) homozygous mutant for w^{1118} (A, J, and J′), $zyx^{\Delta 41}$ (B, K, and K′), $ft^{G\text{-}rv}$ (C, L, and L′), $ft^{G\text{-}rv}$, $zyx^{\Delta 41}$ (D, M, and M′), d^{GC13} (N and N′), d^{GC13}, $zyx^{\Delta 41}$ (O and O′), ex^{e1} (E, P, and P′), ex^{e1}, $zyx^{\Delta 41}$ (F, Q, and Q′), $hpo^{5.1}$ (G, R, and R′), or $hpo^{5.1}$, $zyx^{\Delta 41}$ (H, S, and S′). Retinas are stained with anti-Disc-large (Dlg) to outline cell shape.

(I) Quantification of IOCs for the indicated genotypes ($n \geq 40$). (J′, K′, L′, M′, N′, O′, P′, Q′, R′, and S′) Higher magnification of the respective scanning electron micrographs.

(C–H) and (L)–(S′) represent genotypes generated using the EGUF system in a $zyx^{\Delta 41}$ homozygous background. Scale bars, 20 (A–H) or 50 (J–S′) μm.

single-mutant retinas (Figures 2G and 2I; Table S1). However, these eyes were not visibly less overgrown than $hpo^{5.1}$ single-mutant eyes (Figures 2R–2S′). Removing *zyx* function also moderately suppressed the overgrowth of wing discs carrying the wts^{P2} mutation over a *wts* deficiency (Figures S1S and S1T). Thus, *zyx* is antagonistic to *ex* in tissue growth control, eye differentiation, and animal viability but is only partially required for phenotypes elicited by loss of *ft*, *hpo*, or *wts*.

Zyx Promotes Tissue Growth, and Its Membrane Localization Enhances This Function

We next investigated whether *zyx* is sufficient to promote tissue growth. Overexpressing *zyx* using *nub*-Gal4 significantly increased adult wing size (Figures 3A, 3B, and 3L). *Drosophila* Zyx was shown to localize at the apical epithelial cortex [25], prompting us to test whether this affects its ability to drive growth. As expected, *zyx* variants either tagged with an N-terminal myristoylation signal (myr::Zyx; Figures S2A–S2A‴) or a C-terminal CAAX signal (Zyx::CAAX; Figures S2B–S2B‴) accumulated at the apical cell cortex, with Zyx::CAAX showing a more widespread cortical localization. Strikingly, driving their expression with *nub*-Gal4 strongly enhanced wing growth (Figures 3C, 3D, and 3L), compared to native *zyx* inserted at the same locus (Figures 3B and 3L). In contrast, a *zyx* variant tagged with a mitochondrial targeting signal peptide (*mito::zyx*), which accumulated in punctae (Figures S2C and S2C′), had no effect on wing size (Figures 3E and 3L). Expression of *myr::zyx* under *GMR*-Gal4 also resulted in eye overgrowth (Figures 3F and 3G) and significantly increased IOC numbers (Figures 3H, 3I, and 3M). The overgrowth elicited by Zyx overexpression occurs, at least in part, as a result of increased proliferation, as measured by 5-ethynyl-2′-deoxyuridine (EdU) incorporation to label S-phase entry in

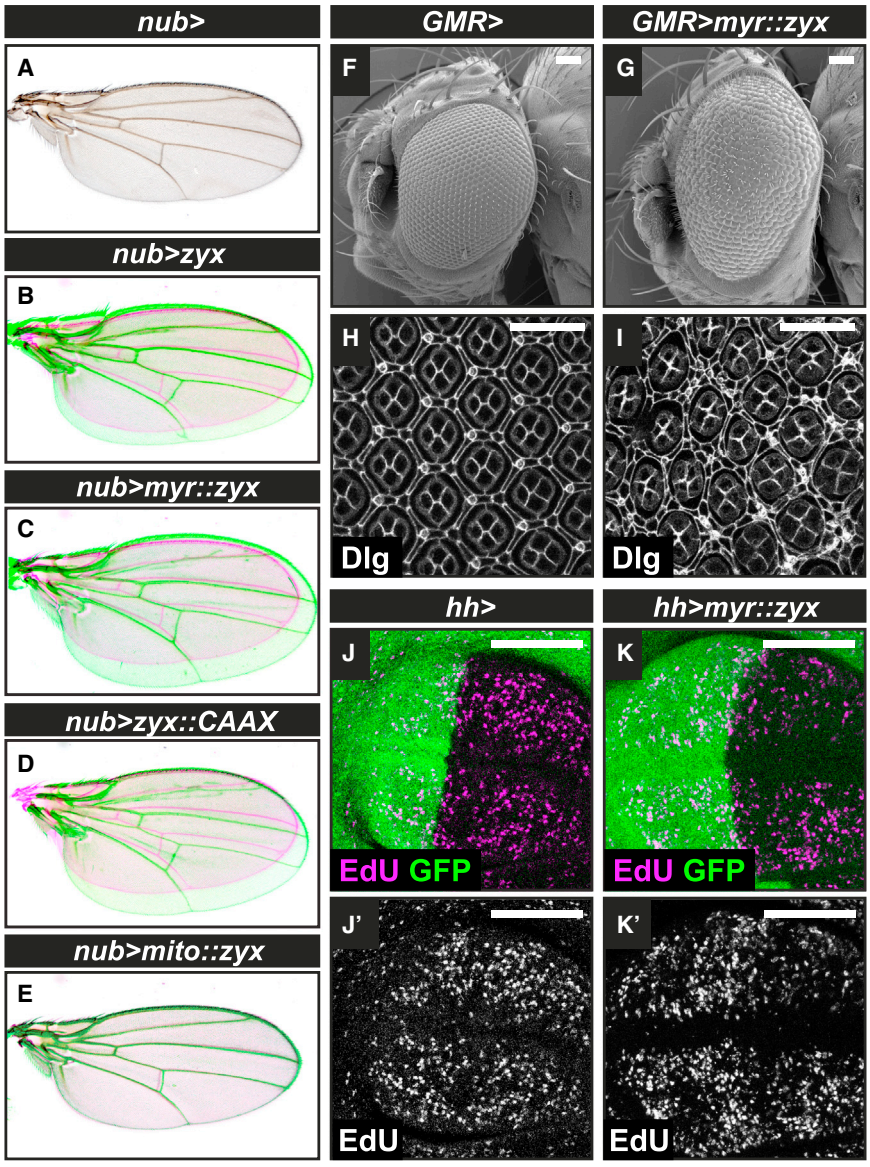

Figure 3. Membrane Targeting of Zyx Promotes Tissue Growth

(A–E) Female wings carrying *nub*-Gal4 (A) and expressing UAS-*zyx* (B), UAS-*myr::zyx* (C), UAS-*zyx::CAAX* (D), or UAS-*mito::zyx* (E).

(F and G) Female adult eyes carrying *GMR*-Gal4 (F) and expressing UAS-*myr::zyx* (G). Scale bars, 50 μm.

(H and I) Female retinas of genotypes shown in (F) and (G) are stained with anti-Dlg to outline cell shape. Scale bars, 20 μm.

(J–K′) Standard confocal sections of third instar wing discs stained with EdU (magenta in J and K; white in J′ and K′) and expressing UAS-*GFP* (J and J′) or UAS-*myr::zyx* (K and K′), under *hh*-Gal4 control. Scale bars, 30 μm.

(L) Quantification of relative wing area normalized to *nub*-Gal4 control for genotypes shown in (A)–(E) ($n \geq 20$).

(M) Quantification of IOC number for genotypes shown in (H) and (I) ($n \geq 40$).

(N) Quantification of EdU signal ratio between posterior and anterior compartments for genotypes shown in (J) and (K) ($n \geq 8$).

myr::zyx-expressing cells in the posterior wing disc compartment (Figures 3J–3K′ and 3N). These observations indicate that Zyx is sufficient to induce cell proliferation and suggest that its localization at apical membrane sites is critical for this function.

Zyx Promotes Yki Target Gene Expression and Enhances the Yki-Sd Interaction

To test whether Zyx-induced overgrowth occurs as a result of Yki activity, we examined the expression of known Yki target genes upon expression of *myr::zyx* or *zyx::CAAX* in the posterior compartment of wing discs [31, 32]. We observed upregulation of *ex-lacZ* (Figures 4A–4B′), *fj-lacZ* (Figures 4C–4D′), and *diap1-GFP* (Figures 4E–4F′). Moreover, the *ban-EGFP* sensor, which is repressed by the *ban* miRNA, was strongly downregulated upon *myr::zyx* expression (Figures 4G–4H″). Additionally, in cultured S2R$^+$ cells, Zyx overexpression activated a *luciferase* reporter driven by a Yki:Gal4 DNA-binding domain fusion protein (Figure 4I) or by a Sd response element (Figure 4J). To investigate if Zyx promotes the interaction between Yki and Sd in vivo, we developed a bi-fluorescence complementation probe (BiFC), where Yki was fused to the YFP N terminus (UAS-*yki::Myc::NYFP*) and Sd fused to the YFP C terminus (UAS-*sd::HA::CYFP*) [33]. Driving *yki::Myc::NYFP* with *sd::HA::CYFP*, using *hh*-Gal4, reconstituted a low and predominantly cytoplasmic YFP signal (Figures 4K, 4K′, and S3D). This enhanced *ex-lacZ* expression in the posterior wing disc compartment (Figures S3A and S3A′), compared to *yki::Myc::NYFP* expression alone (Figures S3A–S3A″) and in contrast to the repressive effect of *sd::HA::CYFP* (Figures S3B–S3B″), thus indicating that the Sd-Yki BiFC probe behaves as a transcriptionally functional Sd-Yki complex. Overexpressing *myr::zyx*

(Figures 4K–4L′ and 4N) or knocking down *wts* (Figures 4K, 4K′, 4M, 4M′, and 4N) significantly increased the average nuclear-cytoplasmic ratio of the YFP signal, compared to discs expressing *mCherry*. However, unlike *wts* depletion, expressing *myr::zyx* under *GMR*-Gal4 control or removing *zyx* function did not affect pYki-S168 in adult head lysates (Figures 4O and 4P). Together, our observations support the notion that Zyx enhances the ability of Yki to interact with Sd and to activate its target genes in a Wts-independent manner.

Zyx Antagonizes Ex Functions in Wing and Eye Development

We investigated the ability of *zyx* (Figures 3B, 5A, 5B, and 5I) to antagonize growth defects caused by overexpression of *ex* (Figures 5C and 5I) or *wts* (Figures 5G and 5I) or a truncated form of *ft* lacking the extracellular domain ($ft^{\Delta ECD}$), which cannot bind Ds and therefore lacks adhesion functions (Figures 5E and 5I) [34]. Wing undergrowth caused by *ex* overexpression was strongly suppressed by *zyx* co-overexpression (Figures 5C, 5D, and 5I), whereas this only mildly alleviated undergrowth of $ft^{\Delta ECD}$-expressing wings (Figures 5E, 5F, and 5I). In contrast, tissue undergrowth caused by *wts* overexpression was not significantly suppressed by increasing Zyx levels (Figures 5G, 5H, and 5I,). These effects were matched by effects on *ex-lacZ* expression, as overexpressing *zyx* in wing discs, using *en*-Gal4, fully restored the reduction of *ex-lacZ* levels resulting from *ex* overexpression (Figures S4C–S4D′) and only partially from $ft^{\Delta ECD}$ (Figures S4E–S4F′) or *wts* overexpression (Figures S4G–S4H′). Thus, consistent with our loss-of-function analysis, *zyx* strongly antagonizes *ex*, while it has milder effects on *ft* and *wts*-induced wing undergrowth. In the eye, *myr::zyx* expression largely suppressed the loss of eye tissue observed upon *ex* overexpression (Figures 5J–5M′), indicating that the antagonism between Zyx and Ex occurs in multiple tissues.

Interestingly, we observed that simultaneous *GMR-Gal4*-driven expression of *myr::zyx* with either *ex* knockdown (Figures S5B, S5B′, and S5I) or *d* overexpression (Figures S5D, S5D′, and S5K), strongly reduced adult eye size and ELAV-positive photoreceptors in eye discs, compared to expression of these constructs alone (Figures S3G, S5A, S5A′, S5C, S5C′, S5F–S5H, and S5J). Simultaneous *ex* knockdown and *d* overexpression did not synergize to reduce adult eye size (Figures S5E and S5E′), nor the number of ELAV-positive photoreceptors in eye discs (Figure S5L), suggesting that *ex* and *d* affect retinal differentiation via distinct mechanisms. We conclude that *zyx* antagonizes *ex* and synergizes with *d* in eye differentiation.

CP and Ena Have Opposite Effects on Zyx-Induced Tissue Growth

We next tested if the barbed-end actin regulators Ena and CP influence Zyx-dependent growth. Strikingly, *GMR*-Gal4 driven co-expression of *myr::zyx* and *ena* led to overgrown eyes (Figures 6A–6D′), showing higher IOC numbers in retinas 40 hr after puparium formation (APF) (Figures 6H and 6I), when compared to the overexpression of either *myr::zyx* or *ena* alone (Figures 6E–6G and 6I). Similarly, *hh*-Gal4 driven overexpression of *zyx::CAAX* and *ena* led to overgrown posterior wing disc compartments compared with expression of *zyx::CAAX* or *ena* alone (Figures S6A–S6E). Overexpressing *ena* with *nub*-Gal4 also led to mild but significant wing overgrowth (Figures S6F, S6H, and S6N) and synergized with *myr::zyx* to induce malformed wings, whose size could not be reliably assessed (Figure S6I).

In contrast, overexpressing the α (*cpa*) and β (*cpb*) subunits of the CP heterodimer reduced wing growth (Figures S6F, S6J, and S6N) and significantly suppressed wing overgrowth induced by *myr::zyx* overexpression (Figures S6G, S6K, and S6N). Conversely, co-expressing *myr::zyx* with a dominant-negative form of CP, lacking the actin-binding domain of Cpa ($cpa^{\Delta ABD}$, *cpb* [35]), resulted in malformed wings, reminiscent of wings overexpressing *myr::zyx* and *ena* (Figure S6M). Expressing *myr::zyx* with $cpa^{\Delta ABD}$, *cpb* also enhanced the number of IOCs in retinas 40 hr APF (Figures S6R and S6S), compared to expressing *myr::zyx* or $cpa^{\Delta ABD}$, *cpb* (Figures S6P, S6Q, and S6S) alone. We conclude that Ena potentiates Zyx-induced tissue growth, while CP counteracts this function.

The Zyx L/FPPPP Motif Is Required to Interact with Ena and Enhances Zyx-Induced Tissue Growth

In vertebrates, ZYX and LPP interact with the EVH1-domain of Ena/VASP proteins via conserved L/FPPPP motifs [26–29]. Accordingly, we were able to co-immunoprecipitate (co-IP) full-length HA-tagged *Drosophila* Zyx with Ena::Flag from S2 cell extracts, while Zyx constructs containing a small truncation that removes the LPPPP motif (aa.209-213 of isoform A) (ZyxΔaa.208-231::HA or ZyxΔaa.208-282::HA) failed to associate with Ena (Figure 6J).

We investigated if the region spanning the LPPPP motif was required for Zyx growth control function. We first compared the ability of Gal4-driven full-length *zyx* or *zyx*Δaa.208-231, inserted at the same locus, to drive wing growth in a $zyx^{\Delta 41}$ mutant background. ZyxΔaa.208-231::EGFP, like full-length Zyx, localized to the apical epithelial cortex (Figures S2D and S2E). However, unlike *zyx* (Figures S6V and S6Y) or *myr::zyx* (Figure S6Y), both untagged and myristoylated *zyxΔaa.208-231* (*myr::zyxΔaa.208-231*) were impaired in their ability to drive wing growth (Figures S6U, S6X, and S6Y). Interestingly, expressing *zyx*Δaa.208-231 with *nub*-Gal4 weakly but significantly reduced wing size (Figures 6K, 6M, and 6Q), suggesting that this form of *zyx* has a mild dominant-negative effect. Moreover, in contrast to wild-type *zyx* (Figures 6L and 6Q), expressing *zyxΔaa.208-231* did not suppress the growth defect of wings overexpressing *ex* under *nub*-Gal4 control but instead reduced wing size even further (Figures 6N, 6P, and 6Q). However, apical Ena levels in the wing disc were not significantly affected upon *zyx* depletion (Figures S7B and S7B′) or *myr::zyx* expression (Figures S7C and S7C′). Thus, although Zyx is not sufficient to localize Ena at the apical cell cortex, the region spanning the L/FPPPP motif of Zyx is required to promote tissue growth and to antagonize Ex function in growth control.

Zyx Antagonizes the Effects of Ex on Apical F-Actin Accumulation

Ex restricts apical F-actin accumulation [19]. Thus, we tested whether Zyx antagonizes the effect of Ex on F-actin accumulation. As expected, knocking down *ex* using *hh*-Gal4 significantly increased the ratio of phalloidin signals between the posterior (experimental) and anterior (control) wing disc compartments (P/A) (Figures 7B, 7B′, and 7H), compared to discs expressing *GFP* (Figures 7D, 7D′, and 7H). This effect was significantly suppressed by *zyx* loss (Figures 7A, 7A′, 7C, 7C′, and 7H). Conversely, overexpressing *ex* reduced the

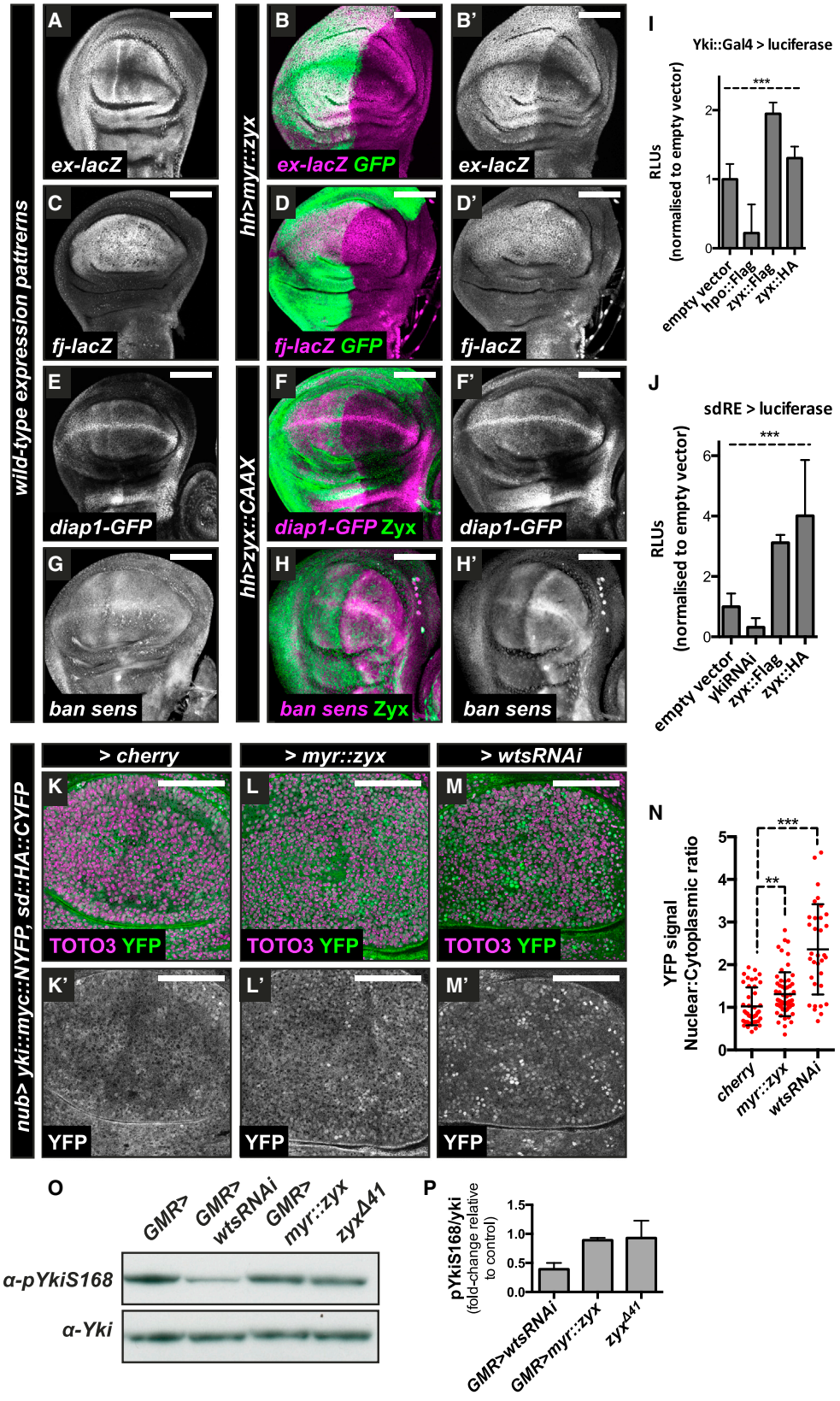

Figure 4. Zyx Enhances Yki Target Gene Expression and Yki-Sd Interaction

(A–H′) Standard confocal sections of third instar wing discs carrying *ex-LacZ* (A–B′), *fj-LacZ* (C–D′), *diap1-GFP* (E–F′; white in E and F′ and magenta in F), or *ban-EGFP* sensor (G–H′), expressing UAS-*GFP* (A, C, E, and G) and UAS-*myr::zyx* (B and B′, and D and D′) or UAS-*zyx::CAAX* (F and F′, and H and H′) under

(legend continued on next page)

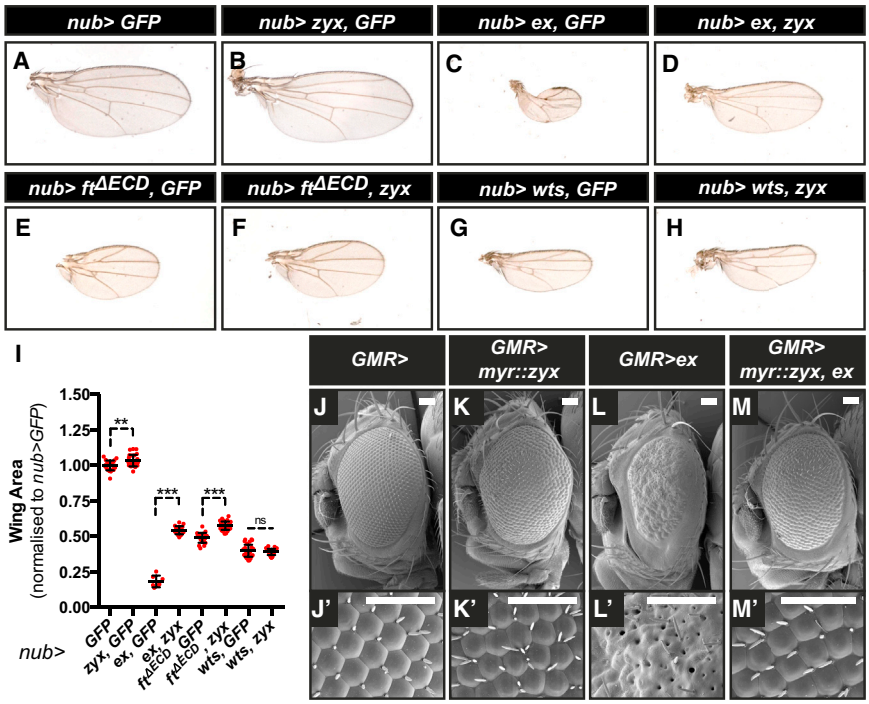

Figure 5. Zyx Antagonizes the Growth-Suppressor Effects of *ex*

(A–H) Female wings expressing UAS-*GFP* (A), *UAS-zyx,* UAS-*GFP* (B), *UAS-ex*, UAS-*GFP* (C), *UAS-ex*, *UAS-zyx* (D), UAS-$ft^{\Delta ECD}$, *UAS-GFP* (E), *UAS-* $ft^{\Delta ECD}$, *UAS-zyx* (F), UAS-*wts*, *UAS-GFP* (G), or *UAS-wts*, *UAS-zyx* (H), under *nub*-Gal4 control.

(I) Quantification of relative wing area normalized to *nub>GFP* for genotypes shown in (A)–(H) ($n \geq 20$).

(J–M′) Female adult eyes carrying *GMR*-Gal4 (J and J′) or expressing UAS-*myr::zyx* (K and K′), UAS-*ex* (L and L′) or UAS-*ex*, UAS-*myr::zyx* (M and M′) under *GMR*-Gal4 control. (J′, K′, L′, and M′) Higher magnification of the respective scanning electron micrographs.

Scale bars, 50 μm.

F-actin P/A ratio (Figures 7F, 7F′, and 7H). This reduction was restored by the co-expression of *zyx::CAAX* (Figures 7G, 7G′, and 7H), although expressing *zyx::CAAX* alone had no detectable effect on F-actin levels (Figures 7E, 7E′, and 7H). The apical localization of Zyx or Ena was not visibly altered in ex^{e1} mutant clones (Figures S7D and S7D′). Conversely, *zyx* depletion did not alter apical Ex levels in the posterior wing disc compartment (Figures S7E and S7E′). In contrast, Ex accumulated at the apical surface of wing discs overexpressing *zyx::CAAX* (Figures S7F and S7F′). This effect is unlikely to result from Ex recruitment by the Crumbs (Crb) polarity complex [36–38], since Crb levels were not affected by *zyx::CAAX* expression (Figures S7G and S7G′). The apical Ex accumulation upon *zyx::CAAX* expression likely results from increased Yki-mediated *ex* transcription (Figures 4B and 4B′). Together, our data support an antagonism between Zyx and Ex based on F-actin regulation, but not through mutual exclusion from the apical cell cortex.

Discussion

In the present study, we have generated a loss-of-function mutation of the *zyx* locus, which revealed that *zyx* is dispensable for viability but is required for normal tissue growth and eye differentiation by antagonizing Ex.

Zyx Antagonizes Ex

Zyx was previously shown to promote Wts degradation in a mechanism based on a Zyx/D interaction [25]. However, we report that *zyx* and *d* have additive effects on tissue growth. In addition, *zyx* loss has a modest effect on *ft* growth phenotypes (Figures 2 and S1), which, in contrast, are highly sensitive to *d* mutations [4, 39], highlighting the possibility of additional functions for Zyx in tissue growth.

Our characterization of the *zyx* mutant shows that Zyx acts in the Ex branch of the Hpo pathway to control tissue growth (Figures 2 and S1). This is in contrast to a previous study using RNAi knockdown of *zyx* and *ex*, which concluded that *zyx* expression had only minor effects on the Ex branch [25]. Our results indicate that *zyx* loss can significantly reverse the lethality and growth defects of *ex* mutant animals (Figures 2 and S1). This antagonistic function of Ex and Zyx is not confined to growth regulation but extends to tissue differentiation. We show that Zyx restricts eye differentiation antagonistically to Ex and in parallel to D but independently of Ft (Figures 2 and S1). Consistent with these observations, simultaneous loss of *ex* and *ft* leads to additive, and therefore apparently independent effects on eye differentiation [40]. Therefore, we propose that Zyx is a key modulator of Ex function.

In growth control, Zyx function may be partially independent of Hpo-Wts signaling, as *zyx* is partially required for the overgrowth of *hpo* and *wts* mutant eye and wing (Figures 2 and S1) but has no major effect on *wts* overexpression in the wing (Figure 5) or Yki phosphorylation by Wts (Figure 4). Ex has been reported to sequester Yki in the cytoplasm

hh-Gal4 control. Discs are stained with anti-β-galactosidase to highlight *lacZ*-reporters (A-D′; magenta in B and D and white in A, B′, C, and D′) or with anti-Zyx (E–H′; green in F and H). Scale bars, 40 μm.

(I and J) Histogram of average relative luciferase units (RLUs) normalized to empty vector, in S2 cell extracts transfected with UAS-*luciferase* and *yki::Gal4DBD* (I) or a *sd* response element (*sdRE*)-*luciferase* reporter (J) for indicated transfections.

(K–M′) Standard confocal sections of third instar wing discs stained with TOTO3 (magenta in K, L, and M) in which *nub*-Gal4 drives the expression of UAS-*yki::Myc::NYFP*, UAS-*sd::HA::CYFP*, and UAS-*mCherry* (K and K′) or UAS-*myr::zyx* (L and L′) or UAS-wtsRNAi9928 (M and M′). Reconstituted YFP signal arising from expressing UAS-*yki::Myc::NYFP* and UAS-*sd::HA::CYFP* (K–M′; green in K, L, and M and white in K′, L′, and M′). Scale bars, 50 μm.

(N) Quantification of nuclear to cytoplasmic YFP signal ratio for genotypes shown in K–M′ ($n \geq 30$).

(O) Western blots on adult head lysates from w^{1118} (lane 1) or expressing UAS-*wts-RNAi* (lane 2) or UAS-*myr::zyx* (lane 3) under *GMR*-Gal4 control or homozygous for $zyx^{\Delta 41}$ (lane 4), blotted with anti-pYkiS168 (upper panel) and anti-Yki (lower panel).

(P) Quantifications of pYkiS168 signals by western blot normalized to corresponding Yki signals for the indicated genotypes (n = 3).

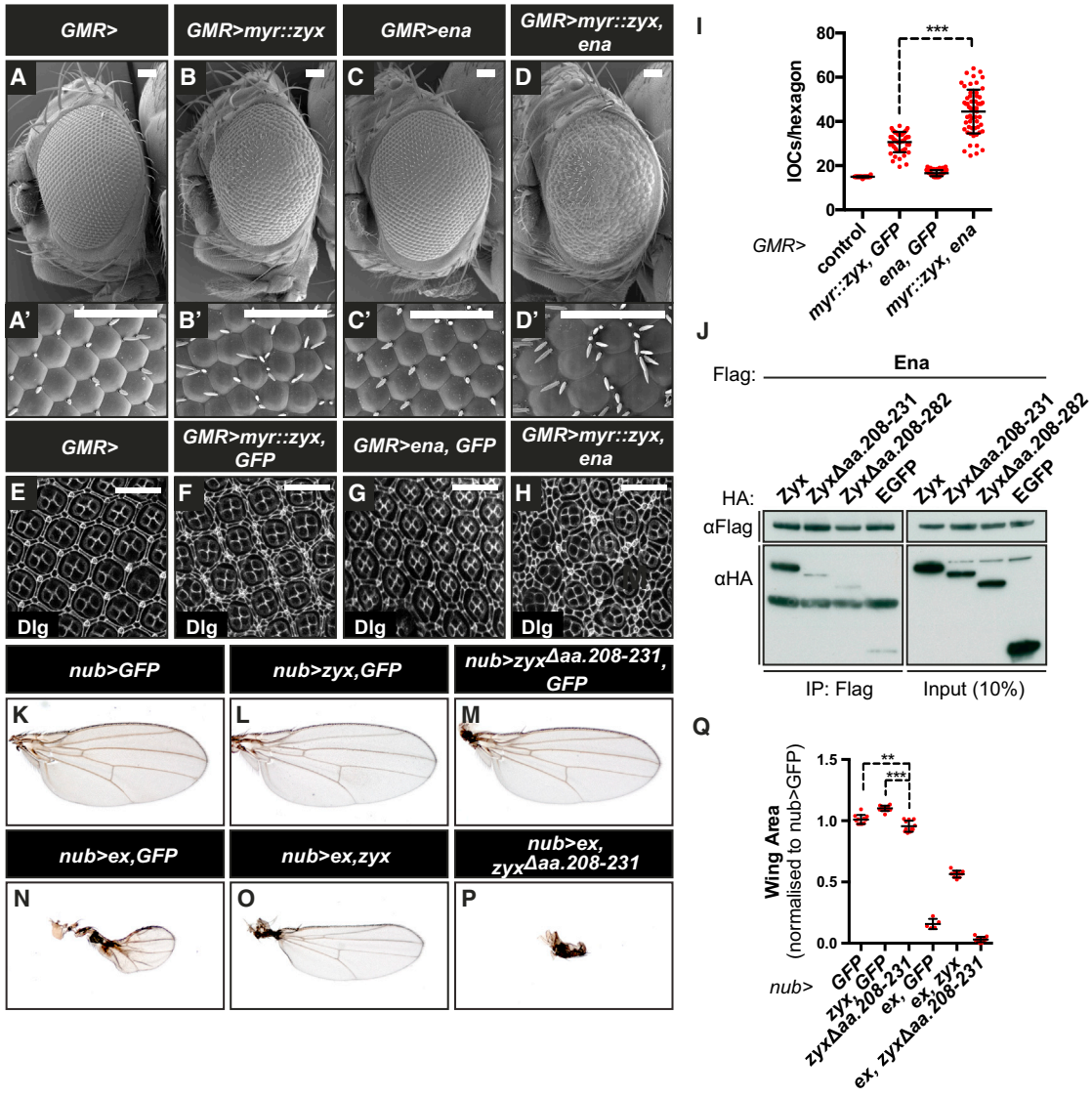

Figure 6. The LPPPP Motif of Zyx Promotes Tissue Growth and Antagonizes Ex

(A–H) Female adult eyes (A–D′) or retinas (E–H) carrying *GMR*-Gal4 (A, A′, and E) and expressing UAS-*myr::zyx* (B, B′, and F) or UAS-*ena* (C, C′, and G) or UAS-*myr::zyx*, UAS-*ena* (D, D′, and H). (A′, B′, C′, and D′) Higher magnification of genotypes shown in (A)–(D). Retinas are stained with anti-Disc-large (Dlg) to outline cell shape. Scale bars, 50 (A–H) and 20 (E–H) μm.

(I) Quantification of IOCs for indicated genotypes ($n \geq 40$).

(J) Flag co-IP from S2 cells lysates expressing Ena::Flag (lanes 1–5) and Zyx::HA (lane 2), ZyxΔaa.208-231::HA (lane 3), Zyx Δaa.208-282::HA (lane 4), or EGFP::HA (lane 5). Blots were probed with anti-Flag or anti-HA. Input represents 10% v/v of lysate used for co-IP.

(K–P) Female adult wings in which *nub*-Gal4 drives expression of UAS-*GFP* (K), UAS-*zyx*, UAS-*GFP* (L), UAS-*zyxΔaa.208-231,* UAS-*GFP* (M), UAS-*ex*, UAS-*GFP* (N), UAS-*ex*, UAS-*zyx* (O), or UAS-*ex*, UAS-*zyxΔaa.208-231* (P).

(Q) Quantification of relative wing area normalized to *nub>GFP* for genotypes shown in (K)–(P) ($n \geq 10$).

through a direct interaction [16, 17]. However, since *ex* mutant overgrowth is suppressed by *zyx* loss (Figures 2 and S1), it is unlikely that Zyx directly antagonizes Ex protein. Instead, we suggest that the interplay between Zyx and Ex in growth control is mediated through their antagonistic effects on F-actin.

Zyx and Yki Regulation by the Actin Cytoskeleton

Our work links F-actin barbed-end polymerization with Zyx/Ex in the control of Yki activity and tissue growth. We show that the Zyx domain encompassing the conserved LPPPP motif, which binds Ena, is required for Zyx to promote growth and to antagonize Ex function (Figures 6 and S6). Moreover, Zyx and Ena synergize to promote tissue growth (Figures 6 and S6). This supports the idea that Zyx promotes tissue growth via its interaction with Ena. Conversely, CP antagonizes Zyx-induced tissue growth (Figure S6) and functions together with Ex in preventing F-actin polymerization [19]. Therefore, an attractive possibility is that antagonistic effects on Yki activity between the activators Zyx/Ena on one hand and the inhibitors Ex and CP on the other hand is played out indirectly through their effects on F-actin polymerization. Consistent with this hypothesis, Zyx antagonizes the effect of Ex on apical F-actin accumulation (Figure 7).

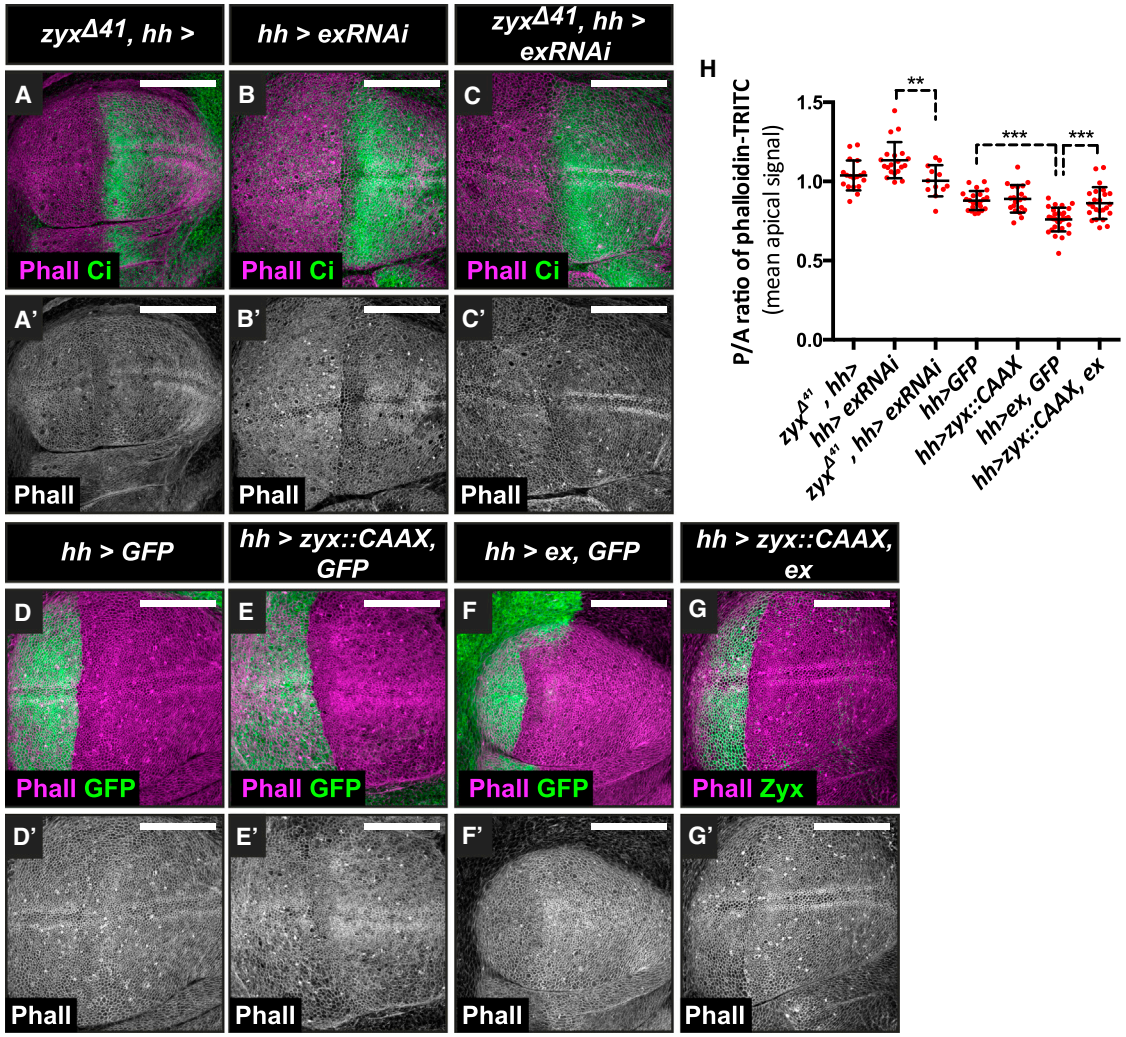

Figure 7. Zyx Antagonizes the Effects of Ex on F-Actin

(A–G′) Standard confocal sections of third instar wing discs stained with phalloidin (Phall; magenta in A, B, C, D, E, F, and G; white in A′, B′, C′, D′, E′, F′, and G′) to mark F-actin and anti-Cubitus interuptus (Ci; green in A, B, and C) to mark anterior wing disc compartments.

(A and A′) *zyx*$^{\Delta 41}$ homozygous mutant bearing *hh*-Gal4.

(B–C′) *hh*-Gal4 driving UAS-*ex-RNAi*^{22994} (B and B′) and homozygous mutant for *zyx*$^{\Delta 41}$ (C and C′).

(D–G′) *hh*-Gal4 driving UAS-*GFP* (D and D′), UAS-*zyx::CAAX*, UAS-*GFP* (E and E′), UAS-*ex,* UAS-*GFP* (F and F′), or UAS-*zyx::CAAX*, UAS-*ex* (G and G′). Scale bars, 30 μm.

(H) Mean intensity ratio between phalloidin signal of posterior and anterior wing compartments for genotypes in (A)–(G′) ($n \geq 15$).

Recent data suggest that the actin cytoskeleton acts in parallel to the core kinase cascade to control YAP/TAZ activity, with CapZ being proposed as one of the "gatekeepers" restricting its nuclear translocation [21]. Yki/YAP/TAZ may respond to the relative activities of Ena and CP, either by being sensitive to the presence of polymerizing actin barbed ends, or because Ena produces a specialized set of cortical actin filaments necessary for Yki/YAP/TAZ activation. The study of the mechanism(s) coupling F-actin and Yki/YAP/TAZ should resolve these issues. We showed that Zyx cortical localization is relevant for its function in promoting tissue growth (Figures 3 and S2). Since Zyx has been shown to rapidly relocalize to strained or severed actin filaments in cultured mammalian cells [41, 42] and *Drosophila* follicular epithelial cells [43], it is possible that Zyx may also link mechanical forces to growth control.

Finally, it is also interesting to note the possible redundancy in growth control between Zyx and other Ena-interacting proteins. Like Zyx, Pico/Lamellipodin contains an EVH1-interacting L/FPPPP motif, and its interaction with Ena promotes tissue growth in *Drosophila* [44]. Since Ena localization is not strictly dependent on Zyx (Figure S7), it is tempting to speculate that Ena recruitment by multiple membrane-associated proteins, such as Zyx and Pico, is a common denominator in the regulation of growth by the actin cytoskeleton.

Experimental Procedures

zyx Mutant Allele

The *zyx*$^{\Delta 41}$ allele was produced by TALEN-mediated mutagenesis (see Supplemental Information). Sequencing confirmed a 7-bp deletion that can be detected with oligonucleotides forward: 5′-CCTCAGCTCTGAGTTGC-3′ and reverse: 5′-GATGAGTTACCGCCACC-3′ (465-bp PCR product). The wild-type *zyx* allele can be discriminated using the oligonucleotides forward: 5′-CTCAGCTCTGAATTCGGAG-3′ and reverse: 5′-GATGAGTTA CCGCCACC-3′ (471-bp PCR product).

Standard Growth Conditions and Analysis of Growth Parameters

For all measurements, flies were left to lay for 24-hr periods, and adults were collected from resulting progeny. For quantification of body weight, batches of 50 female adult flies were pooled. Female adult wings were processed, mounted, and imaged as described in [45]. The average surface area was calculated for each wing outlined separately and including hinge structures, using the *area* function in the ImageJ software. For quantification of IOCs, pupae were staged by collecting white pre-pupae from synchronous test crosses, and retinas were dissected 40 hr after incubation at 25°C. Using the ImageJ software, hexagons connecting the centers of six ommatidia surrounding the ommatidium of interest were outlined and IOCs were quantified for each hexagon, including glial cells and hair cells. Cells straddling the boundary of each hexagon were counted as half-cell. For each genotype, up to ten non-overlapping hexagons from at least five independent retinas were quantified. Statistical significance was analyzed using Student's t test.

Immunohistochemistry

Imaginal discs and retinas were dissected, fixed, and stained according to standard protocols (see Supplemental Information). For S-phase labeling, dissected tissue samples were incubated in 0.01 mM EdU (Invitrogen) and stained using the Click-iT Alexa Fluor 647 cocktail (Invitrogen). F-actin staining was performed using Phalloidin-Tetramethylrhodamine B isothiocyanate conjugate (Phalloidin-TRITC, Sigma), dissolved in methanol, and used at 1:200. EdU and Phalloidin stainings were quantified by the fluorescence intensity averaged across a 50-μm^2 square taken approximately at the center of each quadrant of wing imaginal discs, as defined by the intersection of the dorso-ventral and anterior-posterior compartment boundaries.

Supplemental Information

Supplemental Information includes Supplemental Experimental Procedures, seven figures, and one table and can be found with this article online at http://dx.doi.org/10.1016/j.cub.2015.01.010.

Acknowledgments

We thank the Bloomington *Drosophila* Stock Centre, the National Institute of Genetics, the Developmental Studies Hybridoma Bank, and BestGene, Inc. for their services. We are also grateful to H. McNeill, F. Pichaud, S. Bogdan, J. Colombelli, K. Harvey, G. Halder, and J. Whited for stocks and reagents. We specially thank P. Ribeiro and Y. Zhou for help in producing the modified pKC26 plasmid and P. Ribeiro and Y. Mao for comments on the manuscript. We thank all members of N.T.'s and F.J.'s labs for helpful discussions, M. Russell for advice on scanning electron microscopy, and R. Sadri for helpful molecular biology services. This work was supported by funds from Cancer Research UK (CRUK) to N.T. and from Fundação para a Ciência e Tecnologia (FCT) (PTDC/BIA-BCM/121455/2010) to F.J. P.G. was the recipient of fellowships from FCT (SFRH/BD/47261/2008) and CRUK, and F.J. is the recipient of IF/01031/2012.

Received: August 27, 2014
Revised: December 17, 2014
Accepted: January 2, 2015
Published: February 26, 2015

References

1. Yu, F.X., and Guan, K.L. (2013). The Hippo pathway: regulators and regulations. Genes Dev. *27*, 355–371.
2. Grusche, F.A., Richardson, H.E., and Harvey, K.F. (2010). Upstream regulation of the hippo size control pathway. Curr. Biol. *20*, R574–R582.
3. Hamaratoglu, F., Willecke, M., Kango-Singh, M., Nolo, R., Hyun, E., Tao, C., Jafar-Nejad, H., and Halder, G. (2006). The tumour-suppressor genes NF2/Merlin and Expanded act through Hippo signalling to regulate cell proliferation and apoptosis. Nat. Cell Biol. *8*, 27–36.
4. Cho, E., Feng, Y., Rauskolb, C., Maitra, S., Fehon, R., and Irvine, K.D. (2006). Delineation of a Fat tumor suppressor pathway. Nat. Genet. *38*, 1142–1150.
5. Mao, Y., Rauskolb, C., Cho, E., Hu, W.-L., Hayter, H., Minihan, G., Katz, F.N., and Irvine, K.D. (2006). Dachs: an unconventional myosin that functions downstream of Fat to regulate growth, affinity and gene expression in Drosophila. Development *133*, 2539–2551.
6. Silva, E., Tsatskis, Y., Gardano, L., Tapon, N., and McNeill, H. (2006). The tumor-suppressor gene fat controls tissue growth upstream of expanded in the hippo signaling pathway. Curr. Biol. *16*, 2081–2089.
7. Bennett, F.C., and Harvey, K.F. (2006). Fat cadherin modulates organ size in Drosophila via the Salvador/Warts/Hippo signaling pathway. Curr. Biol. *16*, 2101–2110.
8. Willecke, M., Hamaratoglu, F., Kango-Singh, M., Udan, R., Chen, C.-L., Tao, C., Zhang, X., and Halder, G. (2006). The fat cadherin acts through the hippo tumor-suppressor pathway to regulate tissue size. Curr. Biol *16*, 2090–2100.
9. Thomas, C., and Strutt, D. (2012). The roles of the cadherins Fat and Dachsous in planar polarity specification in Drosophila. Dev. Dyn. *241*, 27–39.
10. Lawrence, P.A., and Casal, J. (2013). The mechanisms of planar cell polarity, growth and the Hippo pathway: some known unknowns. Dev. Biol. *377*, 1–8.
11. Boedigheimer, M., and Laughon, A. (1993). Expanded: a gene involved in the control of cell proliferation in imaginal discs. Development *118*, 1291–1301.
12. McCartney, B.M., Kulikauskas, R.M., LaJeunesse, D.R., and Fehon, R.G. (2000). The neurofibromatosis-2 homologue, Merlin, and the tumor suppressor expanded function together in Drosophila to regulate cell proliferation and differentiation. Development *127*, 1315–1324.
13. Tyler, D.M., and Baker, N.E. (2007). Expanded and fat regulate growth and differentiation in the Drosophila eye through multiple signaling pathways. Dev. Biol. *305*, 187–201.
14. Pellock, B.J., Buff, E., White, K., and Hariharan, I.K. (2007). The Drosophila tumor suppressors Expanded and Merlin differentially regulate cell cycle exit, apoptosis, and Wingless signaling. Dev. Biol. *304*, 102–115.
15. Blaumueller, C.M., and Mlodzik, M. (2000). The Drosophila tumor suppressor expanded regulates growth, apoptosis, and patterning during development. Mech. Dev. *92*, 251–262.
16. Badouel, C., Gardano, L., Amin, N., Garg, A., Rosenfeld, R., Le Bihan, T., and McNeill, H. (2009). The FERM-domain protein Expanded regulates Hippo pathway activity via direct interactions with the transcriptional activator Yorkie. Dev. Cell *16*, 411–420.
17. Oh, H., Reddy, B.V., and Irvine, K.D. (2009). Phosphorylation-independent repression of Yorkie in Fat-Hippo signaling. Dev. Biol. *335*, 188–197.
18. Halder, G., Dupont, S., and Piccolo, S. (2012). Transduction of mechanical and cytoskeletal cues by YAP and TAZ. Nat. Rev. Mol. Cell Biol. *13*, 591–600.
19. Fernández, B.G., Gaspar, P., Brás-Pereira, C., Jezowska, B., Rebelo, S.R., and Janody, F. (2011). Actin-Capping Protein and the Hippo pathway regulate F-actin and tissue growth in Drosophila. Development *138*, 2337–2346.
20. Sansores-Garcia, L., Bossuyt, W., Wada, K., Yonemura, S., Tao, C., Sasaki, H., and Halder, G. (2011). Modulating F-actin organization induces organ growth by affecting the Hippo pathway. EMBO J. *30*, 2325–2335.
21. Aragona, M., Panciera, T., Manfrin, A., Giulitti, S., Michielin, F., Elvassore, N., Dupont, S., and Piccolo, S. (2013). A Mechanical Checkpoint Controls Multicellular Growth through YAP/TAZ Regulation by Actin-Processing Factors. Cell *154*, 1047–1059.
22. Dupont, S., Morsut, L., Aragona, M., Enzo, E., Giulitti, S., Cordenonsi, M., Zanconato, F., Le Digabel, J., Forcato, M., Bicciato, S., et al. (2011). Role of YAP/TAZ in mechanotransduction. Nature *474*, 179–183.
23. Wada, K., Itoga, K., Okano, T., Yonemura, S., and Sasaki, H. (2011). Hippo pathway regulation by cell morphology and stress fibers. Development *138*, 3907–3914.
24. Rauskolb, C., Sun, S., Sun, G., Pan, Y., and Irvine, K.D. (2014). Cytoskeletal tension inhibits Hippo signaling through an Ajuba-Warts complex. Cell *158*, 143–156.
25. Rauskolb, C., Pan, G., Reddy, B.V.V.G., Oh, H., and Irvine, K.D. (2011). Zyxin links fat signaling to the hippo pathway. PLoS Biol. *9*, e1000624.
26. Golsteyn, R.M., Beckerle, M.C., Koay, T., and Friederich, E. (1997). Structural and functional similarities between the human cytoskeletal protein zyxin and the ActA protein of Listeria monocytogenes. J. Cell Sci. *110*, 1893–1906.
27. Drees, B.E., Andrews, K.M., and Beckerle, M.C. (1999). Molecular dissection of zyxin function reveals its involvement in cell motility. J. Cell Biol. *147*, 1549–1560.

28. Drees, B., Friederich, E., Fradelizi, J., Louvard, D., Beckerle, M.C., and Golsteyn, R.M. (2000). Characterization of the interaction between zyxin and members of the Ena/vasodilator-stimulated phosphoprotein family of proteins. J. Biol. Chem. *275*, 22503–22511.
29. Fradelizi, J., Noireaux, V., Plastino, J., Menichi, B., Louvard, D., Sykes, C., Golsteyn, R.M., and Friederich, E. (2001). ActA and human zyxin harbour Arp2/3-independent actin-polymerization activity. Nat. Cell Biol. *3*, 699–707.
30. Stowers, R.S., and Schwarz, T.L. (1999). A genetic method for generating Drosophila eyes composed exclusively of mitotic clones of a single genotype. Genetics *152*, 1631–1639.
31. Saucedo, L.J., and Edgar, B.A. (2007). Filling out the Hippo pathway. Nat. Rev. Mol. Cell Biol. *8*, 613–621.
32. Halder, G., and Johnson, R.L. (2011). Hippo signaling: growth control and beyond. Development *138*, 9–22.
33. Gohl, C., Banovic, D., Grevelhörster, A., and Bogdan, S. (2010). WAVE forms hetero- and homo-oligomeric complexes at integrin junctions in Drosophila visualized by bimolecular fluorescence complementation. J. Biol. Chem. *285*, 40171–40179.
34. Matakatsu, H., and Blair, S.S. (2006). Separating the adhesive and signaling functions of the Fat and Dachsous protocadherins. Development *133*, 2315–2324.
35. Fernández, B.G., Jezowska, B., and Janody, F. (2014). Drosophila actin-Capping Protein limits JNK activation by the Src proto-oncogene. Oncogene *33*, 2027–2039.
36. Robinson, B.S., Huang, J., Hong, Y., and Moberg, K.H. (2010). Crumbs regulates Salvador/Warts/Hippo signaling in Drosophila via the FERM-domain protein Expanded. Curr. Biol. *20*, 582–590.
37. Chen, C.-L., Gajewski, K.M., Hamaratoglu, F., Bossuyt, W., Sansores-Garcia, L., Tao, C., and Halder, G. (2010). The apical-basal cell polarity determinant Crumbs regulates Hippo signaling in Drosophila. Proc. Natl. Acad. Sci. USA *107*, 15810–15815.
38. Ling, C., Zheng, Y., Yin, F., Yu, J., Huang, J., Hong, Y., Wu, S., and Pan, D. (2010). The apical transmembrane protein Crumbs functions as a tumor suppressor that regulates Hippo signaling by binding to Expanded. Proc. Natl. Acad. Sci. USA *107*, 10532–10537.
39. Cho, E., and Irvine, K.D. (2004). Action of fat, four-jointed, dachsous and dachs in distal-to-proximal wing signaling. Development *131*, 4489–4500.
40. Feng, Y., and Irvine, K.D. (2007). Fat and expanded act in parallel to regulate growth through warts. Proc. Natl. Acad. Sci. USA *104*, 20362–20367.
41. Yoshigi, M., Hoffman, L.M., Jensen, C.C., Yost, H.J., and Beckerle, M.C. (2005). Mechanical force mobilizes zyxin from focal adhesions to actin filaments and regulates cytoskeletal reinforcement. J. Cell Biol. *171*, 209–215.
42. Smith, M.A., Blankman, E., Gardel, M.L., Luettjohann, L., Waterman, C.M., and Beckerle, M.C. (2010). A zyxin-mediated mechanism for actin stress fiber maintenance and repair. Dev. Cell *19*, 365–376.
43. Colombelli, J., Besser, A., Kress, H., Reynaud, E.G., Girard, P., Caussinus, E., Haselmann, U., Small, J.V., Schwarz, U.S., and Stelzer, E.H.K. (2009). Mechanosensing in actin stress fibers revealed by a close correlation between force and protein localization. J. Cell Sci. *122*, 1665–1679.
44. Lyulcheva, E., Taylor, E., Michael, M., Vehlow, A., Tan, S., Fletcher, A., Krause, M., and Bennett, D. (2008). Drosophila pico and its mammalian ortholog lamellipodin activate serum response factor and promote cell proliferation. Dev. Cell *15*, 680–690.
45. Ribeiro, P.S., Josué, F., Wepf, A., Wehr, M.C., Rinner, O., Kelly, G., Tapon, N., and Gstaiger, M. (2010). Combined functional genomic and proteomic approaches identify a PP2A complex as a negative regulator of Hippo signaling. Mol. Cell *39*, 521–534.